Supporting Information

Ethane dehydrogenation over Cr/ZSM-5: Characterization of active sites through probe molecule adsorption FTIR

Noah Felvey[1], Michael Meloni[1], Coleman X. Kronawitter[1], Ron C. Runnebaum[1,2*]*

[1]Department of Chemical Engineering, University of California, Davis, CA 95616 USA.

[2]Department of Viticulture & Enology, University of California, Davis, CA 95616 USA

*Correspondence or requests for materials should be addressed to C.X. Kronawitter (ckrona@ucdavis.edu) or R.C. Runnebaum (rcrunnebaum@ucdavis.edu)

Table of Contents

Experimental Details

1. Chemicals

All chemicals were used as received. NH_4-ZSM-5 (CBV 3024E, Zeolyst), 2-propanamine (C_3H_9N, 99+%, Alfa Aesar) chromium (III) acetylacetonate ($Cr(acac)_3$, 99.99%, Sigma-Aldrich), sodium hydroxide (NaOH, ≥97.0%, Sigma-Aldrich), sodium nitrate ($NaNO_3$, 99.0%, Alfa Aesar), calcium nitrate tetrahydrate ($Ca(NO_3)_2{\cdot}4H_2O$, 99+%, Acros Organics), chromium (III) oxide (Cr_2O_3, US Research Nanomaterials), sodium chromate anhydrous (Na_2CrO_4, Fisher Chemical), potassium bromide (KBr, Pike Technologies), aluminum oxide (α-Al_2O_3, 180 micron, >99.7%, Alfa Aesar), nitrogen[a] (N_2, 99.9997%, Airgas), nitrogen[b] (N_2, 99.999%, Praxair), ethane (C_2H_6, 99.999%, Matheson), carbon monoxide (CO, 99.999%, Matheson), hydrogen (H_2, 99.999%, Praxair), nitric oxide (NO, 1%/bal. N_2, Matheson).

[a]Used for DRIFTS experiments

[b]Used for packed-bed reactor

2. Vapor deposition of $Cr(acac)_3$

In previous studies, vapor-phase $Cr(acac)_3$ reacted with SiO_2 surface hydroxyls (silanols) between 200-240 °C, anchoring Cr to the support.[1–3] During calcination, the remaining organic ligands decomposed, leaving Cr^{6+} surface species typical of a Cr/SiO_2 sample with highly dispersed Cr. Similarly, we expected zeolite external surface hydroxyls (external silanols) and bridging hydroxyls (at Al sites) to react with $Cr(acac)_3$, anchoring Cr to the zeolite surface. $Cr(acac)_3$/ZSM-5 mixtures inside vacuum-sealed ampoules were treated at 200 °C and subsequently 300 °C in to ensure quantitative grafting of $Cr(acac)_3$ onto the zeolite. After vapor deposition of $Cr(acac)_3$ under vacuum, samples were calcined in air at 500 °C. TGA-MS analysis of calcination of a 0.5 wt% Cr/H-ZSM-5 sample (Fig. S4) demonstrates that the measured mass loss closely matched the mass loss expected when all Cr is incorporated into the calcined sample. Furthermore, XANES spectra show that after calcination, Cr is mainly present as Cr^{6+} (Fig. S2).

Due to the known surface mobility of Cr under oxidizing conditions at temperatures above 300 °C,[4–6] we expected the location of Cr after calcination to reflect the relative preference of Cr for various binding sites on the zeolite surface, rather than the location where $Cr(acac)_3$ initially grafts during vacuum treatment. In a previous study, Cr was observed by UV-vis spectroscopy to migrate from SiO_2 to alumina (Al_2O_3) and zeolite surfaces.[5] This suggests that Cr may preferentially locate at Al sites in zeolites, rather than defect silanols.

3. Diffuse Reflectance Infrared Fourier Transform Spectroscopy (DRIFTS)

3.1 Probe molecule dosing procedure. All probe molecule experiments were performed isothermally at 30 °C. Initially, the DRIFTS cell contained pure N_2 at 0 psig. Subsequently, 1% NO gas (balance N_2) was flowed into the cell at 30 mL/min with the cell outlet valve closed, thus introducing NO pressure to the cell. After 30 s of flow, the cell inlet valve was closed, sealing the cell containing a known quantity of NO (4.5×10^{-6} mol; this equates to between 3 and 5 moles NO in headspace per mole Cr in sample). Estimating the volume of the cell to be 20 mL, the partial pressure of NO in the cell was 0.55 kPa, before NO adsorption onto the sample. Total pressure is estimated to be 76 kPa-g. Samples were allowed to equilibrate for 10 min after NO dosing, during which time spectra stabilized. To supply a second dose of NO, first the cell pressure was vented quickly through the outlet valve. Next, NO was flowed into the cell

at 30 mL/min for 30 s (with outlet valve closed) before sealing the cell again. The second dose of NO resulted in small increases in all NO peaks, without significant changes to relative peak intensities. A third dose resulted in very little, if any, changes to the DRIFTS spectrum. NO adsorption spectra reported in this study were taken after the second dose of NO. The typical NO adsorption procedure did not include a third dose of NO.

After NO adsorption, the cell pressure was vented through the outlet valve and the cell was purged with pure N_2 flow. After 10 min of 30 mL/min N_2 flow, spectra were fairly stable. The cell outlet valve was closed and 3 mL/min CO diluted in 27 mL/min N_2 was flowed into the cell for 30 s before closing the inlet valve to seal the cell. Again, 10 min equilibration time was allowed for spectra to stabilize before venting the cell and purging with 30 mL/min N_2 flow. Spectra were taken every minute during CO desorption. The small volume of the cell allowed gas phase CO to be removed within one minute, so that adsorbed CO DRIFTS peaks were not obscured by absorbance from gas phase CO.

3.2 Kubelka-Munk (K-M) spectra. All DRIFTS measurements taken in the absence of probe molecules were reported as K-M spectra. A reference reflectance spectrum (R_{KBr}) of dried potassium bromide (KBr) under nitrogen flow was collected by backgrounding the spectrometer. Relative reflectance (R') spectra were calculated by the formula:

$$R' = \frac{R_s}{R_{KBr}}$$

where Rs is the sample reflectance. For small values of R', the Kubelka-Munk function was used to convert relative reflectance to a pseudo-absorbance by the formula:

$$KM = \frac{(1 - R')^2}{2R'}$$

where KM is the Kubelka-Munk function, which is proportional to absorbance for small values of R'. When zeolite samples were measured using KBr as the background, R' is small and the spectra were reported as KM.

3.3 Log inverse reflectance spectra. To measure spectra of adsorption of probe molecules, a background spectrum (R_{bg})of the sample was collected just prior to introduction of the probe gas. Sample spectra were taken after exposure of the sample to probe molecules, and relative reflectance (R') was calculated as:

$$R' = \frac{R_s}{R_{bg}}$$

In this case, the values of R' tended to be close to 1, since the zeolite absorbs strongly compared with the small quantity of adsorbed probe molecules. When R' > 0.6, it was shown previously that the Kubelka-Munk function is not linearly proportional to absorbance.[7] Instead, log inverse reflectance, log(1/R'), is a better approximation of absorbance. Probe molecule spectra were reported in this study as log(1/R').

4. Catalytic Packed-Bed Reactor Measurements

4.1 Experimental setup. The packed-bed reactor consisted of a 6.35 mm OD quartz tube, fitted at either end with ultra-torr compression fittings (Swagelok), flexible stainless-steel tubing (6.35 mm OD)

and quick-connect valves. The valves allowed for sample transfer from the glovebox without exposure to ambient air. In the glovebox, samples were sieved to mesh size 60-40 and loaded into the quartz tube between two lengths of α-alumina powder (2 g each). The purpose of the alumina was to reduce the dead volume of the reactor and situate the catalyst sample at the center of the heated zone of the furnace. The bed, comprised of alumina and catalyst sample, was supported by a small plug of quartz wool.

Stainless steel tubing (1/8" OD) carried all gas flows. Gases were mixed upstream of the reactor, and gas flow rates were controlled by mass flow controllers (Brooks). Three-way valves upstream and downstream of the reactor allowed gas flow to bypass the reactor. Downstream of the reactor, gas lines were heated to 120 °C using heating tape all the way to the GC inlet system, which was heated to 110 °C.

4.2 Gas chromatography (GC). Reactor effluent gas was analyzed by an Agilent 7890a Gas Chromatography unit. Permanent gases detected by TCD were separated using molecular sieve, Porapak Q, and Porapak N columns. A separate channel with N_2 carrier gas and a molecular sieve column was used to detect H_2 by TCD. A third channel measured hydrocarbons by FID. Hydrocarbons were separated using a HP-PLOT Al_2O_3 S column (19095P-S25, Agilent).

4.3 Calculations. The GC was calibrated using a custom gas mix supplied by Matheson (relative accuracy within 2%). Calibration curves were used to convert peak areas to mole fractions. In all experiments, N_2 served as an inert internal standard. All reaction experiments were carried out under the same conditions. A blank reactor experiment was run, measuring 0.059 % ethane conversion for a packed bed of 4 g α-alumina with no catalyst. This value was subtracted from measured ethane conversion before calculating rate of reaction. Ethane conversion was maintained below 10% to achieve a differential reactor yielding accurate reaction rates. In most cases, conversion was kept below 4%. Space velocity was controlled by varying the mass of catalyst in the reactor, keeping flow conditions constant. For time-on-stream data, initial time values (zero TOS) were determined by linear extrapolation from the first two data points measured. Reaction parameters were calculated as follows.

$$ethane\ conversion = \frac{molar\ flow\ rate\ of\ carbon\ (C)\ in\ products}{molar\ flow\ rate\ of\ total\ C\ in\ effluent\ (ethane + products)}$$

$$selectivity, product\ i = \frac{molar\ flow\ rate\ of\ C\ in\ product\ i}{molar\ flow\ rate\ C\ in\ all\ products}$$

$$space\ velocity = \frac{molar\ flow\ rate, ethane\ in\ feed}{moles\ Cr\ in\ packed\ bed}$$

$$rate\ of\ ethane\ conversion = (space\ velocity) \times (ethane\ conversion)$$

Supporting Figures

Fig. S1 X-ray diffraction patterns of H-ZSM-5 and Cr/H-ZSM-5

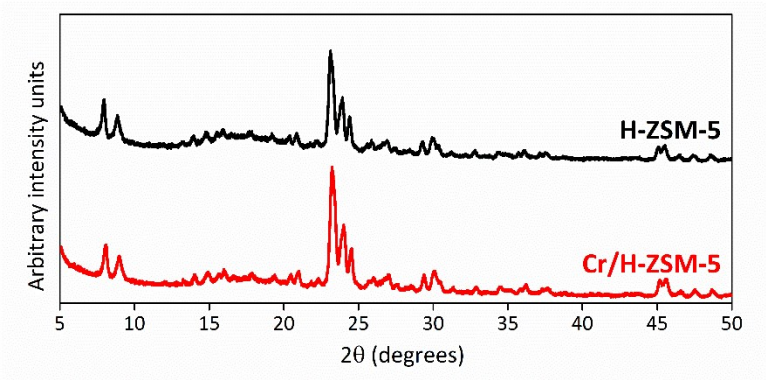

Fig S1. X-ray diffraction patterns for H-ZSM-5 and Cr/H-ZSM-5 (0.10 Cr/Al) after calcination in air at 500 °C. The results verify the crystallinity and presence of the MFI framework structure in both samples. Measurements were performed using a PANalytical X'Pert Pro diffractometer with Cu Kα radiation.

Fig. S2 Brønsted acid site density determined by TPD of 2-propanamine

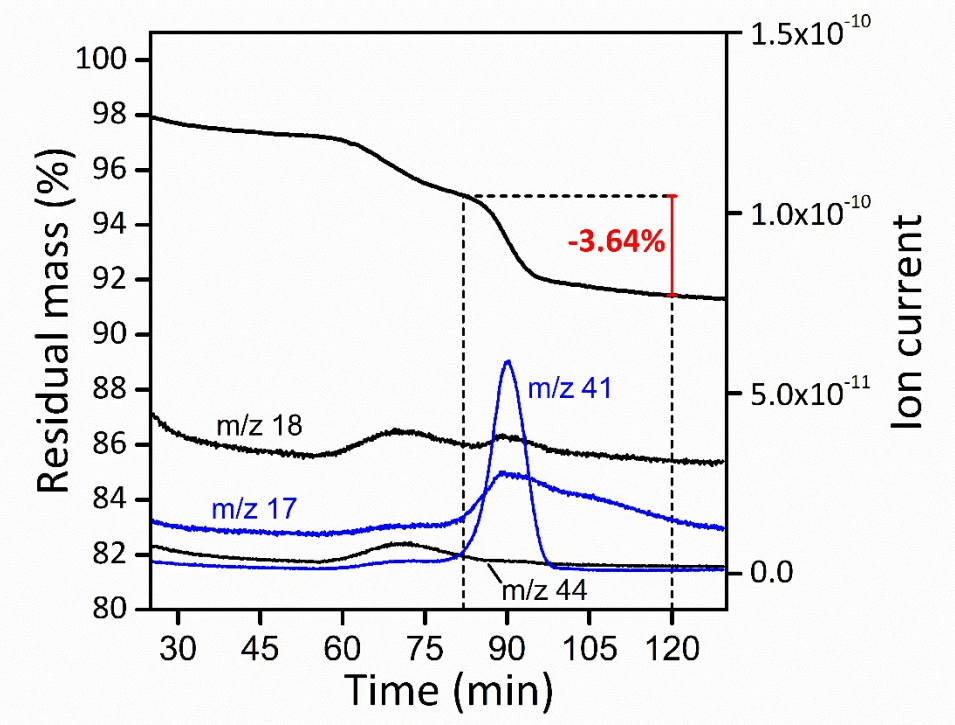

Fig. S2 Temperature-programmed desorption of 2-propanamine. Mass spectrum signals at m/z 41 and m/z 17 correspond to propene and ammonia, respectively, which form and desorb following decomposition of 2-propanamine on Brønsted acid sites at around 300-350 °C.[8] The molar amount of 2-propanamine that decomposes corresponds to an equivalent molar amount of Brønsted acid sites in the zeolite. From this experiment, the Brønsted acid site density was calculated to be 616 µmol/g, consistent with previously determined values.[9, 10]

Fig. S3 N_2 adsorption isotherms of selected samples

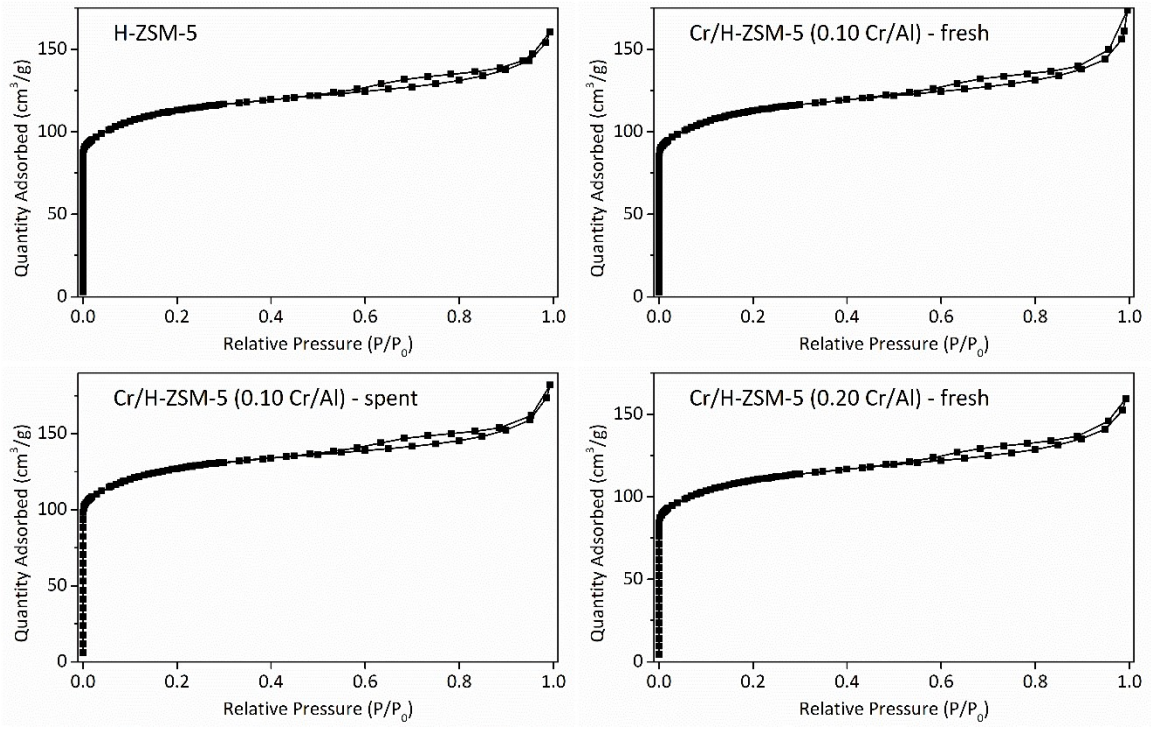

Fig. S3 N_2 adsorption isotherms collected at -196 °C. Calculated surface areas and pore volumes are shown in Table S1. Isotherms for H-ZSM-5 and fresh Cr/H-ZSM-5 samples were collected after calcination. Isotherm for spent Cr/H-ZSM-5 (0.10 Cr/Al) was collected after sample was used for ethane dehydrogenation at 650 °C for 3 hours, operating at ca. 4% ethane conversion. All samples were degassed under vacuum at 300 °C for 3 hours before N_2 adsorption.

Fig. S4 DRIFTS hydroxyl region of H-ZSM-5 and Na-ZSM-5

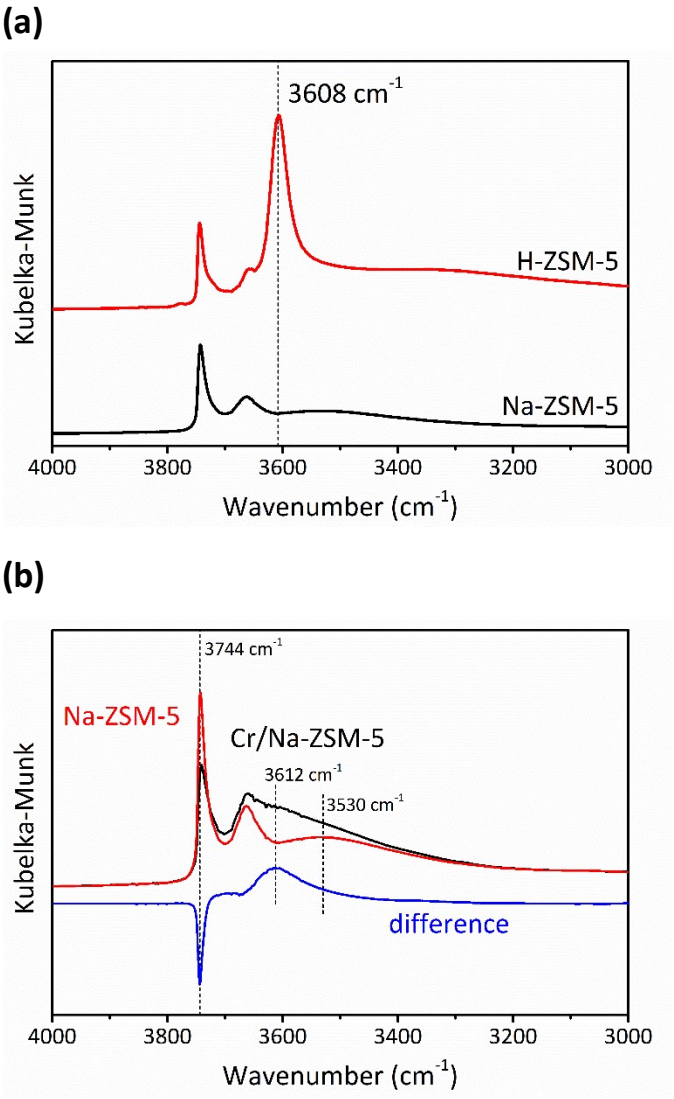

Fig. S4 **(a)** DRIFTS spectra in the OH region of calcined supports H-ZSM-5 and Na-ZSM-5 before Cr deposition. Spectra were taken at 100 °C under N_2 flow after samples were treated at 650 °C for 1 hour under flowing N_2. These spectra demonstrate that Na-exchange of H-ZSM-5 caused disappearance of the peak at 3608 cm^{-1} due to zeolite bridging hydroxyls (Al-OH-Si).[11] No significant change to external silanol (3744 cm^{-1}) and extra-framework Al hydroxyl (3658 cm^{-1} and 3777 cm^{-1}) peaks[11, 12] was observed. **(b)** DRIFTS spectra in the OH region of Na-ZSM-5 (red) after 30-minute treatment in N_2 at 300 °C, Cr/Na-ZSM-5 (black) after reduction in CO at 300 °C, and the difference spectrum (blue). Spectra were taken at 100 °C under N_2 flow and normalized by the intensity of the zeolite Si-O-Si overtone peak at 1987 cm^{-1}. Significant decrease in intensity of the 3744 cm^{-1} band due to external silanols (SiOH) after Cr loading suggests that Cr resides largely at external silanol sites. The band at 3530 cm^{-1} due to internal silanols ("silanol nests")[12] does not change significantly with Cr loading, as is seen in the difference spectrum. This demonstrates that silanol nests are not the dominant binding site for Cr in Cr/Na-ZSM-5, although it does not rule out the possibility that a fraction of Cr present does replace Si in framework defect silanol nests. The increase

in intensity at 3612 cm^{-1} is difficult to assign. The broadness of the difference peak suggests that this could be due to perturbation of silanols by Cr or a small amount of moisture. It could also be explained by the formation of a small amount of bridging hydroxyls (Al-OH-Si). It has also been shown that bridging hydroxyls (Cr-OH-Si) can form when Cr replaces vacant framework T sites,[13] but a definitive assignment of the resulting O—H stretching band in FTIR has not been made.

Fig. S5 XANES spectra of fresh, reduced Cr/ZSM-5 samples

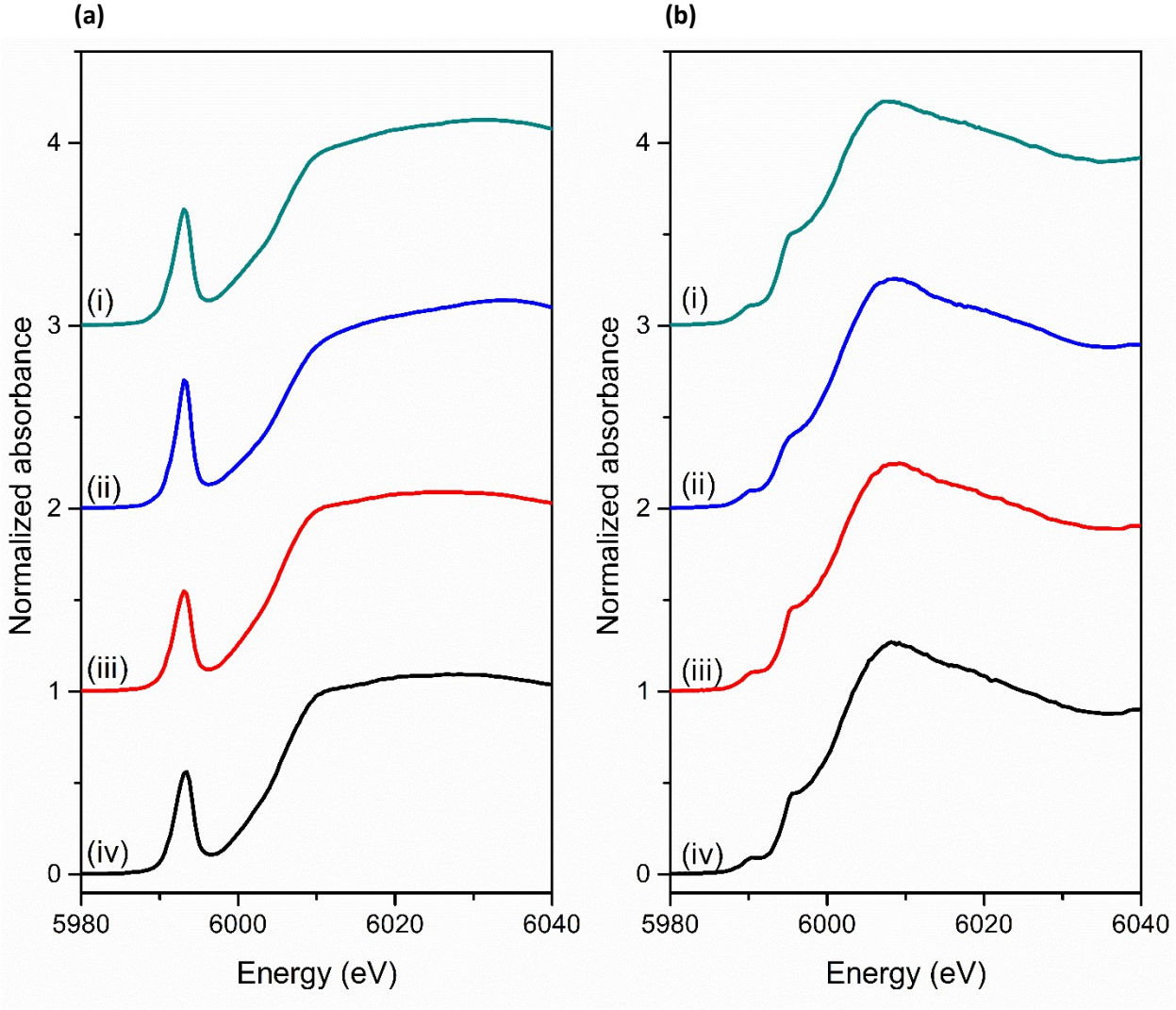

Fig. S5 Samples legend below. **(a)** XANES spectra of fresh samples after calcination. Spectra were taken at room temperature under helium flow. In all samples, an intense pre-edge peak at 5993 eV indicates that Cr is present predominantly as tetrahedral Cr^{6+} species.[14, 15] This peak is also present in the spectrum of Na_2CrO_4 in Fig. S3. **(b)** XANES spectra of samples from Fig. S2(a) after reduction at 300 °C in 10% CO (bal. N_2) for 30 min. Spectra were taken at 300 °C under 10% CO flow. Shifting of the edge to ca. 6002 eV and appearance of pre-edge features at 5988, 5990, and 5995 eV suggest the presence of mainly Cr^{2+} in all samples after reduction.[14, 15] However, the presence of a minority of Cr in higher oxidation states cannot be ruled out.

Samples:

(i) 0.10 Cr/Al Cr/Ca-ZSM-5

(ii) 0.10 Cr/Al Cr/Na-ZSM-5

(iii) 0.10 Cr/Al Cr/H-ZSM-5

(iv) 0.17 Cr/Al Cr/H-ZSM-5

Fig. S6 XANES spectra of reference compounds

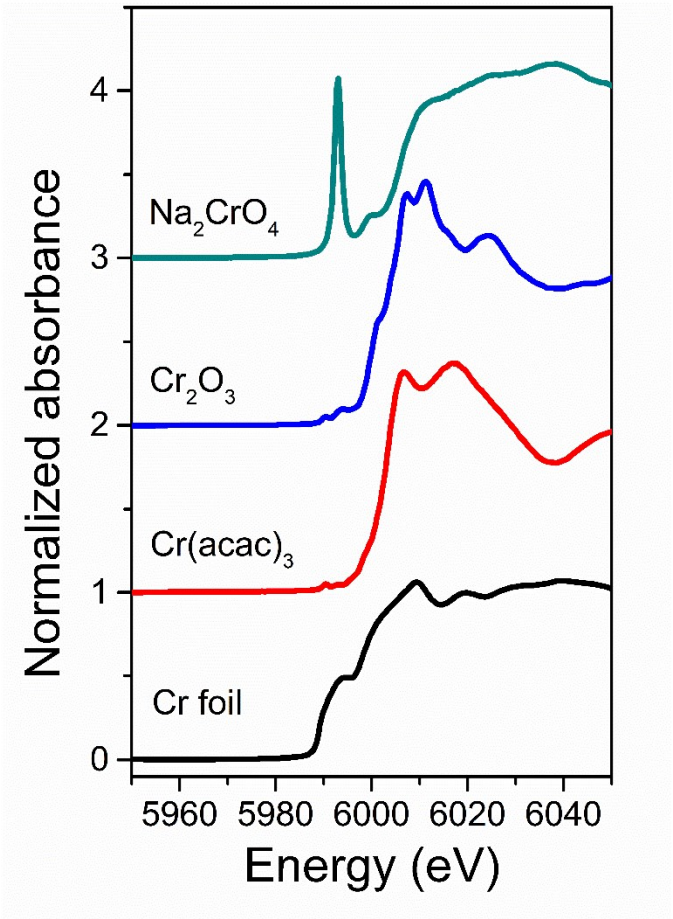

Fig. S6 XANES spectra of reference compounds taken under ambient air at room temperature.

Fig. S7 TGA, calcination of $Cr(acac)_3$/H-ZSM-5

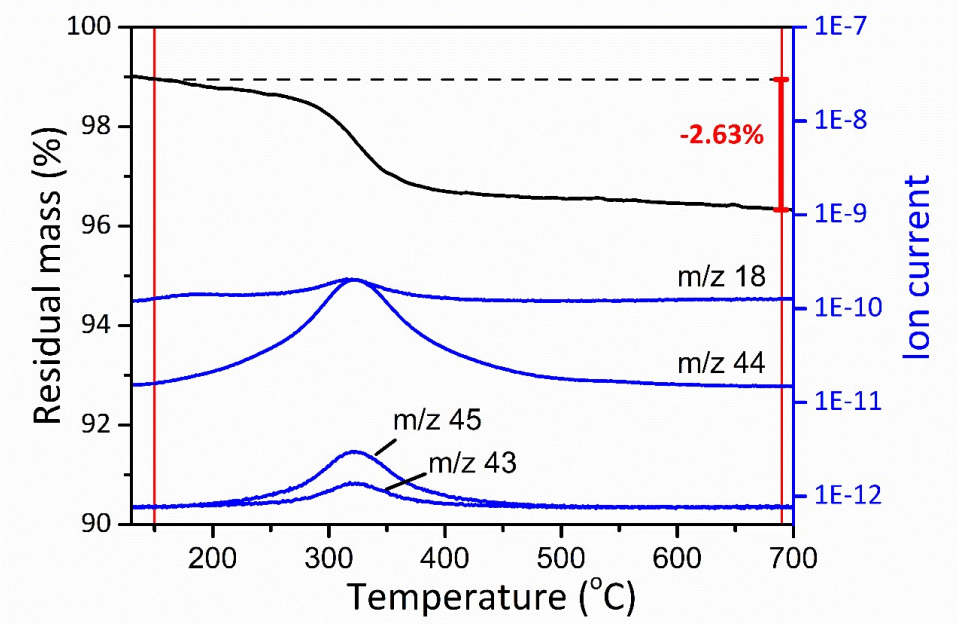

Fig. S7 TGA-MS calcination of $Cr(acac)_3$/H-ZSM-5 mixture used for preparation of 0.10 Cr/Al Cr/H-ZSM-5. Isothermal soak at 120 °C for one hour removed adsorbed water that accumulated on the sample during transfer to the TGA. Mass loss during desorption of carbon-containing products is labelled. Mass spectrometer signals for water (m/z 18) and CO_2 (m/z 44) were the major signals observed. Signals for m/z 45 and m/z 43 were also observed, as previously reported.[2] Acetylacetone, acetic acid, and acetone display major fragments at m/z 43. Acetic acid displays a major fragment at m/z 45. No deviation from baseline was observed at mass m/z 151, a major fragment of $Cr(acac)_3$.

This sample was prepared by vacuum heat treatment of a mixture of 18.15 mg $Cr(acac)_3$ and 500.5 mg H-ZSM-5. Assuming all Cr remains on the zeolite surface during calcination and is converted from $Cr(acac)_3$ to $Cr^{6+}(=O)_2$, the expected mass loss during calcination is calculated as:

$$mol\ Cr\ in\ sample = \frac{(18.15\ mg)}{(MW_{Cr}\ g/mol) \times (1000\frac{mg}{g})} = 5.20 \times 10^{-5}\ mol\ Cr$$

$$expected\ mass\ loss\ (mg) = (mol\ Cr) \times \left(MW_{Cr(acac)3}\frac{g}{mol} - MW_{CrO2}\frac{g}{mol}\right) \times \left(1000\frac{mg}{g}\right) = 13.79\ mg$$

$$expected\ \%\ mass\ loss = \frac{(expected\ mass\ loss, mg)}{18.15\ mg + 500.5\ mg} = 2.66\%$$

Where MW_i denotes molar weight of component i.

The close correspondence of the measured mass loss to the expected mass loss demonstrates that all Cr is incorporated into the sample during vacuum treatment and calcination.

Fig. S8 TGA, calcination of spent 0.10 Cr/Al Cr/Na-ZSM-5

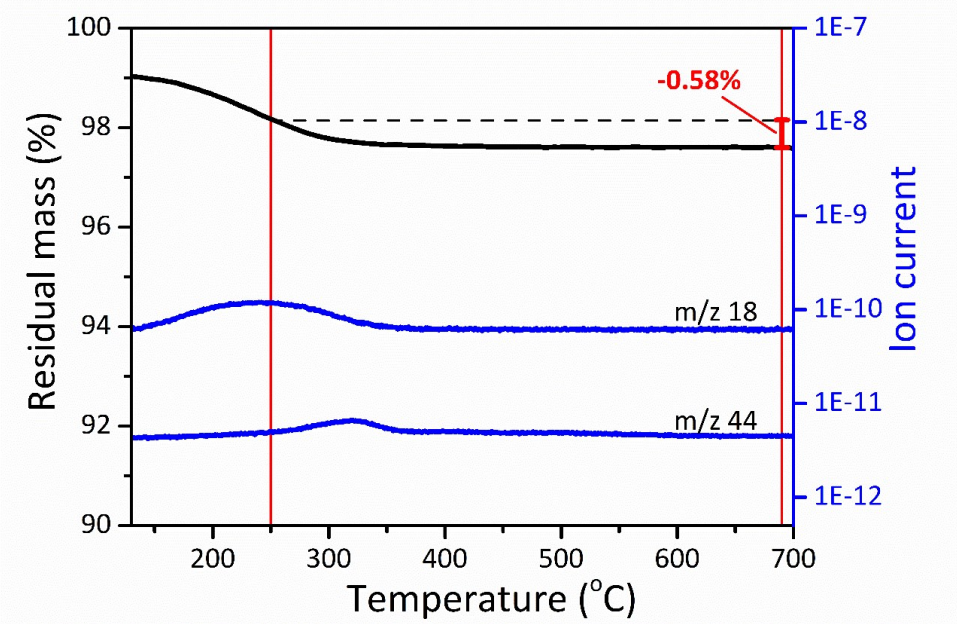

Fig. S8 TGA-MS decoking of spent 0.10 Cr/Al Cr/Na-ZSM-5. Prior to decoking, catalyst was used for ethane dehydrogenation at 650 °C for three hours operating at 3% initial ethane conversion. Sample was cooled under N_2 flow and loaded to the TGA. After one-hour isothermal at 120 °C to remove moisture adsorbed to the sample after exposure to ambient lab air, TGA furnace was ramped at 5 °C/min with synthetic air flow to combust deposited carbon from the sample. The mass spectrometry signal for CO_2 (m/z 44) was used to identify carbon combustion. The mass loss due to coke is labelled on the figure.

Fig. S9 TGA, calcination of spent 0.10 Cr/Al Cr/H-ZSM-5

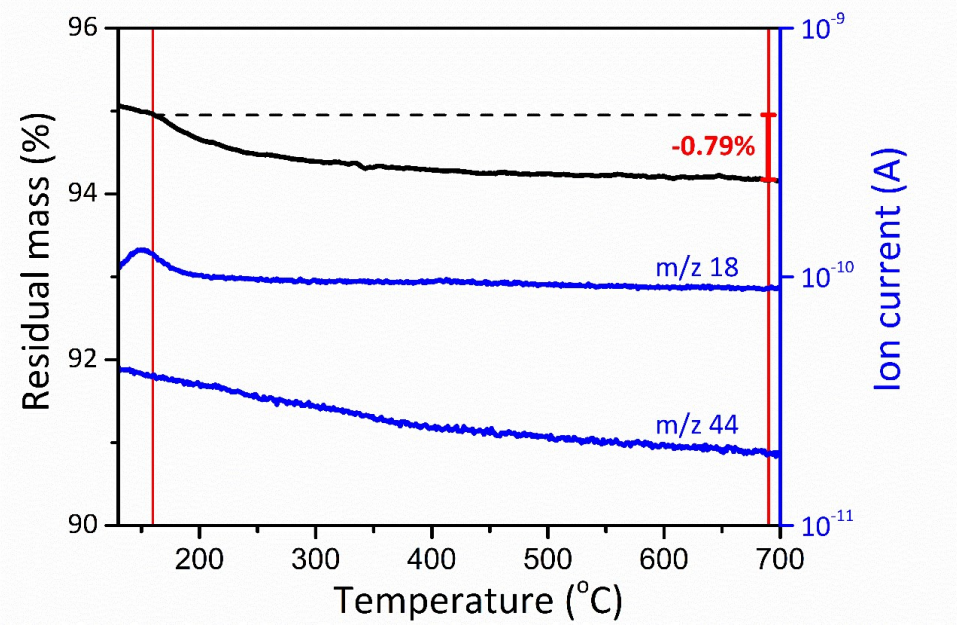

Fig. S9 TGA-MS decoking of spent 0.10 Cr/Al Cr/H-ZSM-5. Prior to decoking, catalyst was used for ethane dehydrogenation at 650 °C, operating at 4% ethane conversion for three hours. Sample was cooled under N_2 flow and loaded to the TGA. After one-hour isothermal at 120 °C to remove moisture adsorbed to the sample after exposure to ambient lab air, TGA furnace was ramped at 5 °C/min with synthetic air flow to combust deposited carbon from the sample. The mass spectrometry signal for CO_2 (m/z 44) was used to identify carbon combustion. Baseline m/z 44 signal was slightly high during this experiment due to the use of pure CO_2 flow in a previous experiment run on the instrument. The temperature range used to determine mass loss was taken to be the same as that used in Fig. S7. The mass loss due to coke is labelled on the figure.

Fig. S10 TGA, calcination of spent 0.17 Cr/Al Cr/H-ZSM-5

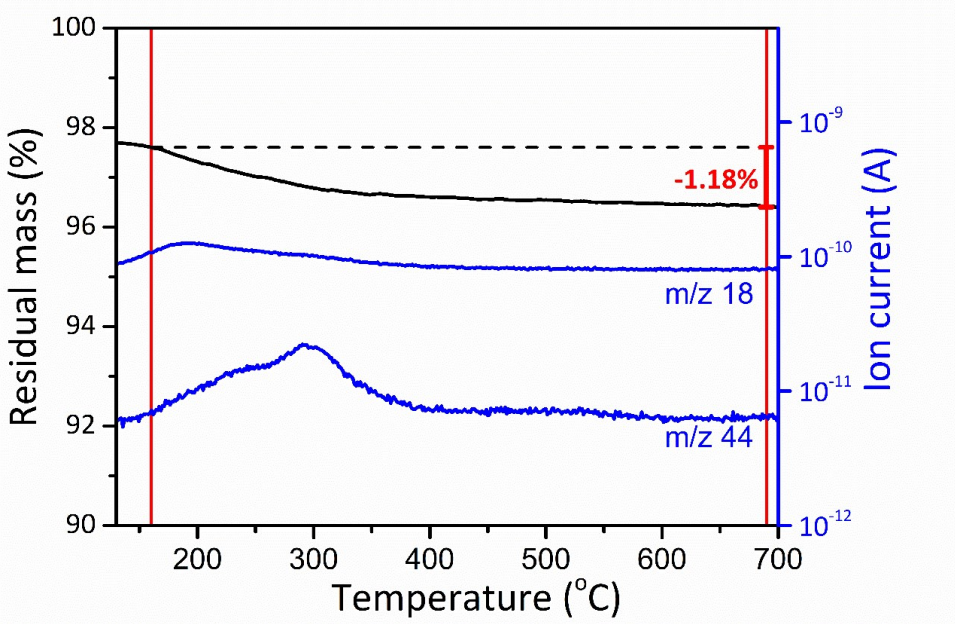

Fig. S10 TGA-MS decoking of spent 0.17 Cr/Al Cr/H-ZSM-5. Prior to decoking, catalyst was used for ethane dehydrogenation at 650 °C, operating at 4% ethane conversion for 3 hours. Sample was cooled under N_2 flow and loaded to the TGA. After one-hour isothermal at 120 °C to remove moisture adsorbed to the sample after exposure to ambient lab air, TGA furnace was ramped at 5 °C/min with synthetic air flow to combust deposited carbon from the sample. The mass spectrometry signal for CO_2 (m/z 44) was used to identify carbon combustion. The mass loss due to coke is labelled on the figure.

Fig. S11 DRIFTS spectrum of NO adsorption onto 0.10 Cr/Al Cr/H-ZSM-5

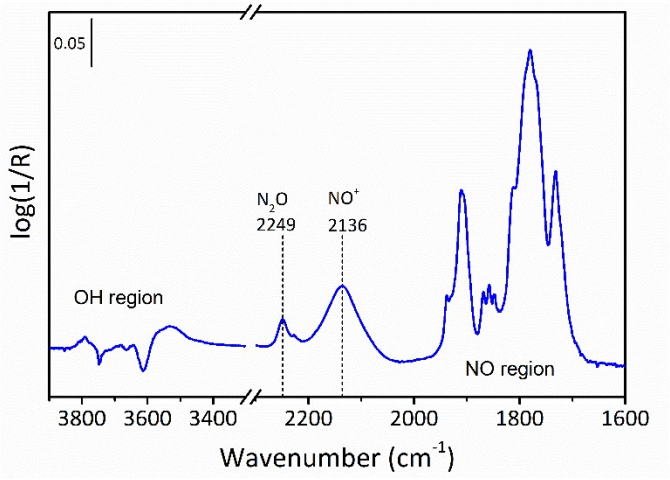

Fig. S11 DRIFTS spectra of NO adsorption at 30 °C on 0.10 Cr/Al Cr/H-MFI after treatment for one hour at 650 °C under N_2 flow. Peaks due to N_2O (2249 cm^{-1}) and NO^+ (2136 cm^{-1}) were observed during NO adsorption.[12]

Fig. S12 DRIFTS spectrum of NO adsorption onto H-ZSM-5

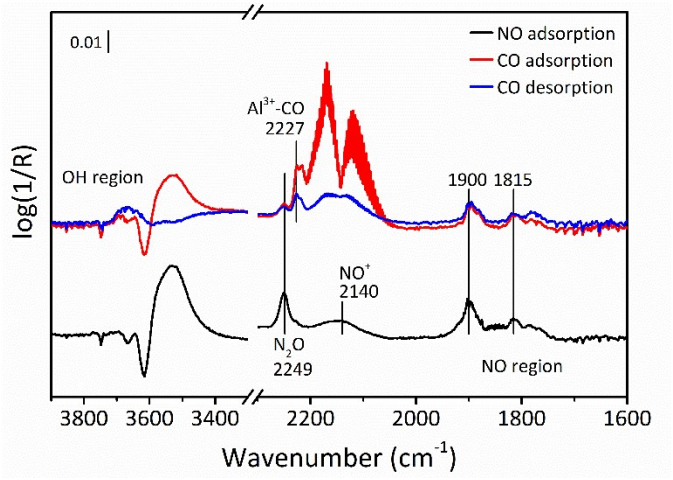

Fig. S12 DRIFTS spectra of NO and CO adsorption at 30 °C on H-MFI after treatment for one hour at 650 °C under N_2 flow. Black curve: spectrum taken under static NO pressure. Red curve: spectrum taken after NO purge and introduction of static CO pressure. Blue curve: spectrum taken after one minute of purging CO from cell with 30 mL/min N_2.

Only very small peaks appeared in the nitrosyl region (see scale bar to compare with other samples). In the carbonyl region, only peaks at ca. 2227 cm^{-1}, characteristic of extra-framework Al^{3+} carbonyls, were observed.[12]

Fig. S13 DRIFTS spectra of NO/CO adsorption onto Cr/Na-ZSM-5

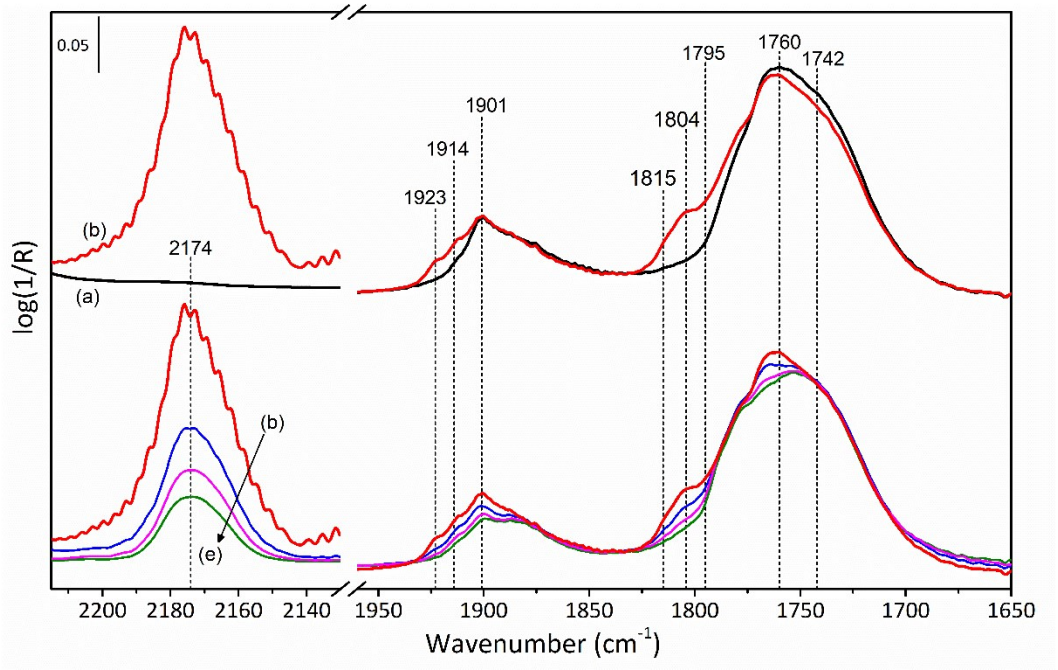

Fig. S13 DRIFTS spectra of NO and CO adsorption at 30 °C on 0.10 Cr/Al Cr/Na-ZSM-5 after treatment for one hour at 650 °C under 10% H_2 flow (bal. N_2). **(a)** Spectrum taken under static NO pressure. **(b)** Spectrum taken after venting NO and introducing static CO pressure. **(c)-(e)** Spectra taken while cell was purged with N_2 flow. N_2 purge was not performed prior to CO dosing.

In contrast to Cr/H-ZSM-5 and Cr/Ca-ZSM-5 samples, no isosbestic point in the NO region was observed during CO desorption. This indicates that Cr dinitrosyl species in Cr/Na-ZSM-5 were unstable, as they were destroyed upon brief N_2 purge.

Fig. S14 DRIFTS spectra of NO/CO adsorption onto Cr/Ca-ZSM-5

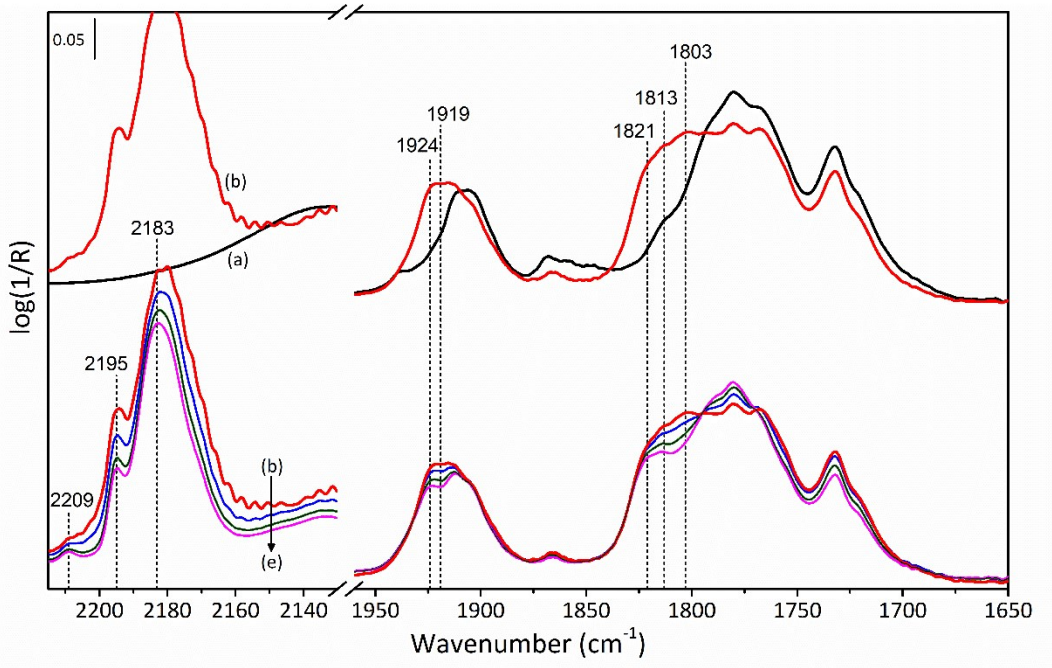

Fig. S14 DRIFTS spectra of NO and CO adsorption at 30 °C on 0.10 Cr/Al Cr/Ca-ZSM-5 after treatment for one hour at 650 °C under 10% H_2 flow (bal. N_2). **(a)** Spectrum taken under static NO pressure. **(b)** Spectrum taken after venting NO and introducing static CO pressure. **(c)-(e)** spectra taken while cell was purged with N_2 flow. N_2 purge was not performed prior to CO dosing.

Isosbestic point at ca. 1795 cm^{-1} in spectra (b)-(e) indicates desorption of CO restores Cr-dinitrosyl species.

Fig. S15 Initial TOF adjusted for support activity, versus Cr/Al

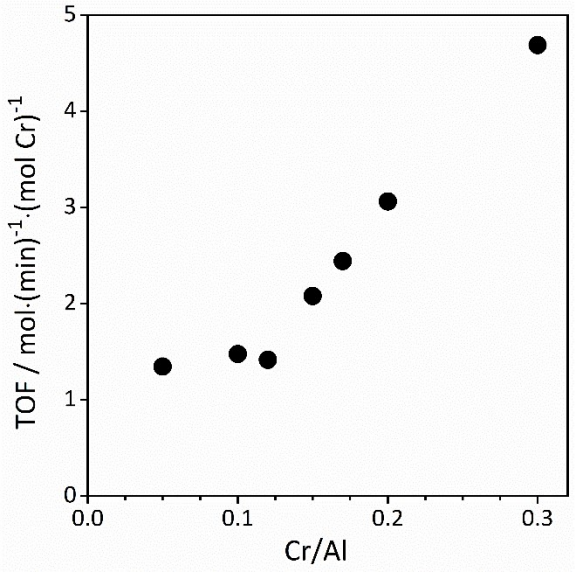

Fig. S15 Turnover frequency (TOF) of ethane conversion, adjusted for contribution of acid catalysis by zeolite Brønsted acid sites. Measured ethane conversion values were adjusted by subtracting the conversion measured for an equivalent mass of blank H-ZSM-5 (0.013% conversion per mg). This adjusted conversion value was used to calculate adjusted TOF.

Fig. S16 Comparison of 0.30 Cr/Al Cr/H-ZSM-5 deactivation at different ethane conversion levels

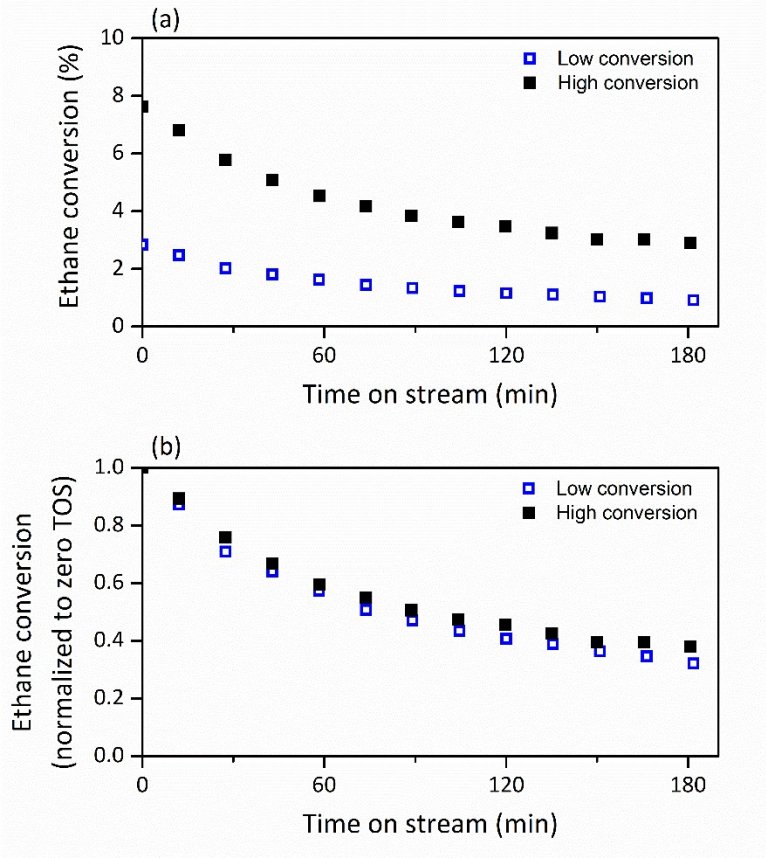

Fig. S16 **(a)** Time on stream ethane conversion (650 °C) for 0.30 Cr/Al Cr/H-MFI. Two separate experiments were performed at different conversion, which was controlled by the mass of catalyst in the bed. **(b)** Time on stream ethane conversion, normalized by initial value, for the same experiments as in panel (a).

The rate of deactivation was not influenced by ethane conversion, suggesting that increasing partial pressure of products (i.e. ethylene) was not the primary cause for deactivation.

Fig. S17 Comparison of 0.10 Cr/Al Cr/M-ZSM-5 (M = H, Na, Ca) – Ethane conversion, NO-DRIFTS

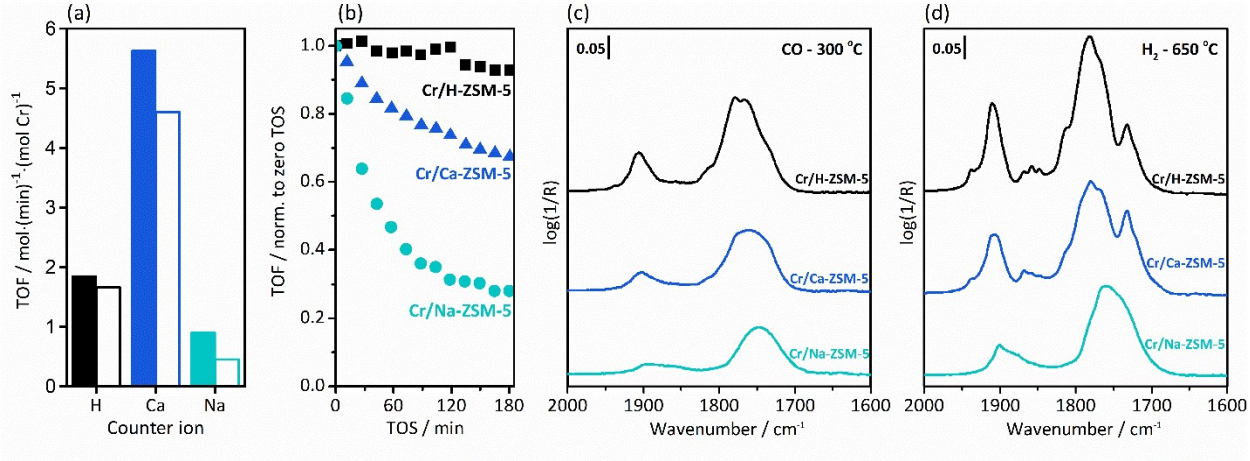

Fig. S17 Comparison of 0.5 wt% Cr/H-ZSM-5, 0.5 wt% Cr/Ca-ZSM-5, and 0.5 wt% Cr/Na-ZSM-5 catalysts. **(a)** Rate of ethane conversion at zero time on stream (full bars) and after one hour on stream (open bars). **(b)** Normalized rate of ethane conversion as a function of time-on-stream. **(c)** FTIR spectra of NO adsorbed at 30 °C after reduction in CO at 300 °C. **(d)** FTIR spectra of NO adsorbed at 30 °C after reduction in H_2 at 650 °C.

Supporting Tables

Table S1. Summary of surface area measurements

	H-ZSM-5	0.10 Cr/Al Cr/H-ZSM-5 - fresh	0.10 Cr/Al Cr/H-ZSM-5 - spent	0.20 Cr/Al Cr/H-ZSM-5 - fresh
BET surface area (m^2/g)	420.1	409.6	474.5	408.8
Micropore surface area (m^2/g)	313.0	302.8	336.0	281.2
External surface area (m^2/g)	107.1	106.8	138.5	127.7
Micropore volume (cm^3/g)	0.128	0.127	0.136	0.114

Table S2. Summary of ethane dehydrogenation catalysis data

	Cat. Mass	Zero time on stream*				One hour on stream*			
	(mg)	X_{C2H6}	S_{C2H4}	S_{CH4}	S_{C3}	X_{C2H6}	S_{C2H4}	S_{CH4}	S_{C3}
H-ZSM-5	32.0	0.72	66.8	21.4	10.8	0.65	68.3	8.86	6.39
0.10 Cr/Al Cr/Na-ZSM-5	22.1	1.16	99.6	0.44	-	0.57	99.3	0.75	-
0.10 Cr/Al Cr/Ca-ZSM-5	26.4	8.68	95.5	1.82	1.90	7.09	96.3	1.44	1.56
0.10 Cr/Al Cr/H-ZSM-5	26.5	2.81	94.5	3.04	2.05	2.59	94.8	2.94	1.94
0.05 Cr/Al Cr/H-ZSM-5	44.4	2.66	88.5	6.85	4.31	2.50	89.3	6.40	3.97
0.12 Cr/Al Cr/H-ZSM-5	21.4	2.59	95.7	2.42	1.55	2.44	95.8	2.31	1.48
0.15 Cr/Al Cr/H-ZSM-5	21.9	4.41	96.7	1.53	1.24	4.56	96.7	1.53	1.22
0.17 Cr/Al Cr/H-ZSM-5	14.6	3.57	97.5	1.03	0.87	3.54	97.5	1.02	0.87
0.20 Cr/Al Cr/H-ZSM-5	16.1	6.05	97.2	1.03	1.05	5.18	97.4	0.97	0.96
0.30 Cr/Al Cr/H-ZSM-5	8.8	7.48	97.3	0.86	1.05	4.53	98.6	0.50	0.40
0.30 Cr/Al Cr/H-ZSM-5	2.4	2.84	98.3	0.57	0.50	1.63	98.8	0.54	0.25

*X_{C2H6} = % conversion ethane; S_i = % selectivity to product(s) i

Reactor conditions: T = 650 °C; P = 3 psig; flow rates: 4 sccm ethane, 44 sccm N_2.

	Previously reported bands (cm^{-1})[11, 12, 16–19]					
	Cr/SiO_2	**Cr/Al_2O_3**	**Cr/SiO_2-TiO_2**	**Cr-H-ZSM-5**	**Cr/silicalite-1**	**Cr/Si-Beta**
	Ref [16]	Ref [17]	Ref [18]	Ref [11]	Ref [19]	Ref [12]
ν_s/ν_{as}, $Cr^{2+}(NO)_2$	1865/1747, 1880/1755	1880/1755	1856/1742, 1868/1736	1902/1768	1860-1875/1745	1883**/1755**
ν_s/ν_{as}, $Cr^{3+}(NO)_2$		1905/1775	1875/1755	1910/1782		
ν_{N-O}, $Cr^{2+/3+}$-NO	1810-1815	1940, 1875, 1820	1807	1890, 1815, 1782	1800	1794

Table S3. Previously reported Cr-nitrosyl band assignments

**Cr oxidation state unknown

	Previously reported bands (cm^{-1})[16, 19]	
	Cr/SiO_2 Ref [19]	**Cr/SiO_2** Ref [16]
$Cr^{2+}(NO)_2$	1856/1743	1865/1747, 1880/1755
$Cr^{2+}(NO)_3$	1862*/1845*/1745*	
$NO^{\delta+}$ in $Cr^{2+}(NO)_4$	1908*/1885*/1875*	
$NO^{\delta-}$ in $Cr^{2+}(NO)_4$	1725*, 1700*	
$Cr^{2+}(NO)_2(CO)$	2180†*, 2170†*, 1880*/1760*	2179†, 1886/1760
$Cr^{2+}(NO)_2$(pyridine)		1850/1702
Cr^{2+}(NO)(pyridine)		1710, 1725

Table S4. Previously reported nitrosyl and mixed-ligand band assignments for Cr/SiO_2

*adsorption at liquid nitrogen temperature
†carbonyl band

Table S5. Cr nitrosyl and carbonyl bands observed in this study

	Observed bands (cm^{-1})		
	Cr/H-ZSM-5	**Cr/Na-ZSM-5**	**Cr/Ca-ZSM-5**
$Cr^{2+}(NO)_2$	1904/1767, 1869/1732	1860-1880/1747	1904/1767, 1869/1732
$Cr^{n+}(NO)_2$	1911/1780	1900/1760	1911/1780
Cr^{n+} - NO	1789		1789
$Cr^{2+}(NO)_2(CO)$	2182†/1921/1809	2174†, 1912, 1804	2183†/1919/1813
$Cr^{n+}(NO)_2(CO)$	2195†/1926/1821	1921, 1814	2195†/1924/1821
Unassigned nitrosyl bands	1938, 1930, 1858, 1848, 1814, 1720		1803

†carbonyl band

References

1 I. V. Babich, Y. V. Plyuto, P. Van Der Voort and E. F. Vansant, *J. Colloid Interface Sci.*, 1997, **189**, 144.

2 A. Hakuli and A. Kytökivi, *Phys. Chem. Chem. Phys.*, 1999, **1**, 1607.

3 B. M. Weckhuysen, R. Ramachandra Rao, J. Pelgrims, R. A. Schoonheydt, P. Bodart, G. Debras, O. Collart, P. Van Der Voort and E. F. Vansant, *Chem. - Eur. J.*, 2000, **6**, 2960.

4 B. M. Weckhuysen, I. E. Wachs and R. A. Schoonheydt, *Chem. Rev.*, 1996, **96**, 3327.

5 B. M. Weckhuysen, B. Schoofs and R. A. Schoonheydt, *J. Chem. Soc., Faraday Trans.*, 1997, **93**, 2117.

6 M. P. McDaniel, K. S. Collins and E. A. Benham, *J. Catal.*, 2007, **252**, 281.

7 J. Sirita, S. Phanichphant and F. C. Meunier, *Anal. Chem.*, 2007, **79**, 3912.

8 G. Kofke, R. J. Gorte and W. E. Farneth, *J. Catal.*, 1988, **114**, 34.

9 A. J. Jones, R. T. Carr, S. I. Zones and E. Iglesia, *J. Catal.*, 2014, **312**, 58.

10 O. A. Abdelrahman, K. P. Vinter, L. Ren, D. Xu, R. J. Gorte, M. Tsapatsis and P. J. Dauenhauer, *Catal. Sci. Technol.*, 2017, **7**, 3831.

11 M. Mihaylov, A. Penkova, K. Hadjiivanov and M. Daturi, *J. Mol. Catal. A: Chem.*, 2006, **249**, 40.

12 K. Hadjiivanov, A. Penkova, R. Kefirov, S. Dzwigaj and M. Che, *Microporous Mesoporous Mater.*, 2009, **124**, 59.

13 J. Janas, J. Gurgul, R. P. Socha, J. Kowalska, K. Nowinska, T. Shishido, M. Che and S. Dzwigaj, *J. Phys. Chem. C*, 2009, **113**, 13273.

14 E. Groppo, C. Lamberti, S. Bordiga, G. Spoto and A. Zecchina, *Chem. Rev.*, 2005, **105**, 115.

15 M. Botavina, C. Barzan, A. Piovano, L. Braglia, G. Agostini, G. Martra and E. Groppo, *Catal. Sci. Technol.*, 2017, **7**, 1690.

16 E. Garrone, G. Ghiotti, C. Morterra and A. Zecchina, *Z. Naturforsch., B: J. Chem. Sci.*, 1987, **42**, 728.

17 J. B. Peri, *J. Phys. Chem.*, 1974, **78**, 588.

18 S. J. Conway, J. W. Falconer and C. H. Rochester, *J. Chem. Soc., Faraday Trans.*, 1989, **85**, 79.

19 A. Zecchina, G. Spoto, G. Ghiotti and E. Garrone, *J. Mol. Catal.*, 1994, **86**, 423.